Proceedings of the
44th IEEE Conference on Decision and Control, and
the European Control Conference 2005
Seville, Spain, December 12-15, 2005

Optimal control of drug delivery to brain tumors for a test of PDE driven models using the Galerkin finite element method *

Siddhartha P. Chakrabarty† and Floyd B. Hanson†

Abstract— **The Galerkin finite element method is used to examine the a simple polar test case of optimal drug delivery to brain tumors. The PDE driven mathematical model is a system of three coupled reaction diffusion equations involving the tumor cells, the normal tissue and the drug concentration. An optimal control problem is formulated keeping in mind the primary goals of the treatment, i.e., minimizing the tumor cell density and reducing the side effects of drugs. A distributed parameter method based on application of variational calculus to a pseudo-Hamiltonian, is used to obtain a coupled system of forward state equations and backward co-state equations. The Galerkin form of the finite element method is used due to its greater facility in numerically representing complex structures such as those in the brain. Finally, a two-dimensional circular disk test case is considered and partitioned into a set of rectangular finite elements in polar coordinates with bilinear basis functions on each element, except that triangular elements are used to accommodate the singular origin. Results show significant reduction of the tumor density over time.**

I. Introduction

Over the years, various kinds of cancerous growth have been studied from the mathematical point of view. One such kind is the growth of brain tumors. A brain tumor, like other cancerous cells, originates from a cell that proliferates and starts affecting the neighboring normal cells. As time progresses the tumor cell becomes malignant and takes life threatening proportions. Understanding the mechanisms that augment and abet the growth of tumors is necessary for formulating an optimal treatment. The most commonly occurring form of brain tumors are the gliomas, which account for a majority of the reported cases. Gliomas are notoriously invasive and infiltrate the surrounding tissues [6], [8]. Despite the availability of advanced diagnostic tools like computerized tomography (CT) scan and magnetic resonance imaging (MRI), realistic treatment options have been limited. One major impediment in the treatment of brain tumors has been the inability of the drugs to penetrate the *blood brain barrier (BBB)*[2]. The *BBB* is a desirable natural protection that exists in the human brain to prevent water soluble toxic materials from entering the central nervous system. The two most commonly used forms of drug delivery are drugs conjugated with a polymer and delivery by optimal distribution of drugs about the original tumor site. Wang et al. [9], [10] have worked extensively on drug delivery to tumors in three dimension for drugs like IgG and BCNU. While this paper was motivated by a biomedical problem, the treatment here will be mostly mathematical. We will focus primarily on control for the optimal distribution of the drug about the original tumor site. While a lot of work targets study of solid tumors, our primary concern would be the post operative treatment, *i.e,* the resection that occurs after the surgeon has removed the bulk of the tumor. The mathematical model used in this paper is taken from Chakrabarty and Hanson [1], which was influenced by the models of Gatenby et al. [3] and Mansuri [5]. Both of these papers, while not dealing directly with brain tumors, have models which closely resemble the growth of brain tumors. Murray's book [6] is an excellent reference for different types of growth mechanisms. Westman et al. [11] look at three common kinds of tumor growth, viz., exponential, logistic and Gompertz. In the next section we take a fairly generalized model which could be used in the mathematical study of other biomedical phenomena. Further, an optimal control problem is formulated keeping in mind the primary goals of the treatment, i.e., minimizing the tumor cells and reducing the side effects of drugs. We define a *pseudo-Hamiltonian* and use the necessary conditions from calculus of variations [4]. This leads to a coupled system of forward state equations and backward co-state equations, but the main thrust of this paper is to formulate a finite element numerical scheme to solve for this set state and co-state vector equations.

II. Mathematical Model

In the PDE driven, *distributed parameter control* model of Chakrabarty and Hanson [1], the tumor cell and normal cell density and the drug concentration at any position vector $\mathbf{x}$ and time $t \in [0, t_f]$, in the *interior* Ω of the domain, denoted by $n_1(\mathbf{x}, t)$, $n_2(\mathbf{x}, t)$ and $c(\mathbf{x}, t)$ respectively, are taken as the state variables. Defining the global state vector as

$$\mathbf{Y}(\mathbf{x}, t) \equiv \begin{bmatrix} n_1(\mathbf{x}, t) & n_2(\mathbf{x}, t) & c(\mathbf{x}, t) \end{bmatrix}^\top, \tag{1}$$

the governing nonlinear vector PDE is given by

$$\mathbf{Y}_t(\mathbf{x}, t) = D\nabla_x^2[\mathbf{Y}] + (A + B)(\mathbf{Y})\mathbf{Y} + \mathbf{U}, \tag{2}$$

where $D = [D_i\delta_{i,j}]_{3\times 3}$,

$$A(\mathbf{Y}) = a_1(1 - Y_1/k_1)\mathbf{e}_1\mathbf{e}_1^\top + a_2(1 - Y_2/k_2)\mathbf{e}_2\mathbf{e}_2^\top - a_3\mathbf{e}_3\mathbf{e}_3^\top,$$

$$B(\mathbf{Y}) = -(\alpha_{1,2}Y_2 + \kappa_{1,3}Y_3)\mathbf{e}_1\mathbf{e}_1^\top - (\alpha_{2,1}Y_1 + \kappa_{2,3}Y_3)\mathbf{e}_2\mathbf{e}_2^\top,$$

$$\mathbf{U}(\mathbf{x}, t) = U_3(\mathbf{x}, t)\mathbf{e}_3. \tag{3}$$

*The work is supported by the National Science Foundation under Grant DMS-02-07081. The content of this material is that of the authors and does not necessarily reflect the views of the National Science Foundation.. The first author was also supported by the *Provost's Award for Graduate Research* awarded by the Graduate College at the University of Illinois at Chicago.

†Department of Mathematics, Statistics, and Computer Science, University of Illinois at Chicago 851 S Morgan St.; m/c 249, Chicago, IL 60607-7045, USA, E–Mail: pratim@math.uic.edu and hanson@math.uic.edu

0-7803-9568-9/05/$20.00 ©2005 IEEE

Here, $D_i > 0$ is the ith diffusion coefficient (could be inhomogeneous depending on the brain matter [8]; in this case the $\nabla_x \cdot D\nabla_x$ should replace the $D\nabla_x^2$ for the diffusion operator; D_1 is mainly metastatic and D_2 should be negligible since normal), $A_{i,i}(Y_i)Y_i$ is the ith growth rate (logistic for $i = 1:2$ and exponentially decaying for $i = 3$, but they can be purely exponential, logistic or Gompertzian [6] depending the type of growth stage), $\alpha_{i,j}$ are per capita logistic death rates due to competition, $\kappa_{i,j}$ are the death rates due to treatment and $u = u(\mathbf{x}, t)$ is the rate at which the drug is being delivered and will be the control variable in an optimal control system. Also, $\mathbf{e}_i$ is the ith unit vector. The initial conditions and the no-flux boundary conditions on the boundary $\partial\Omega$ are, respectively,

$$\mathbf{Y}(\mathbf{x}, 0) = \mathbf{Y}_0(\mathbf{x}), \text{ and } -D(\widehat{\mathbf{N}} \cdot \nabla_x)[\mathbf{Y}](\mathbf{x}, t) = \mathbf{0}. \quad (4)$$

III. The Optimal Control Problem

The objective functional in the quadratic form of running and terminal cost is given by,

$$J[\mathbf{Y}, \mathbf{U}] = \frac{1}{2}\int_0^{t_f} dt \int_\Omega d\mathbf{x} \left(\mathbf{Y}^\top R\mathbf{Y} + (\mathbf{U}-\mathbf{U}_0)^\top S\,(\mathbf{U}-\mathbf{U}_0)\right) + \frac{1}{2}\int_\Omega d\mathbf{x}\,(\mathbf{Y}^\top Q\mathbf{Y})(\mathbf{x}, t_f), \quad (5)$$

where $R = \tilde{r}_1 \mathbf{e}_1\mathbf{e}_1^\top$, $S = s_3\mathbf{e}_3\mathbf{e}_3^\top$, $Q = q_1\mathbf{e}_1\mathbf{e}_1^\top + q_3\mathbf{e}_3\mathbf{e}_3^\top$ and $\mathbf{U}_0 = U_{0,3}(\mathbf{x}, t)\mathbf{e}_3$. The goal is to minimize this functional with respect to the drug input rate relative to some threshold rate $U_{0,3}$ and the terminal costs at t_f, i.e., $\min_u [J(u)]$. Note that here $\tilde{r}_1 > 0$ is the tumor burden cost coefficient and $s_3 > 0$ is the drug delivery cost coefficient, while $q_1 > 0$ and $q_3 > 0$ are final costs. We are trying to minimize the density of tumor cells and the drug delivery quadratic control term $(U_3(\mathbf{x}, t) - U_{0,3}(\mathbf{x}, t))^2$. Also, the goal at the final time t_f is to minimize the final tumor density and more importantly the drug concentration so as to reduce the effects of toxicity. In addition, no assumption is made about the control constraints, even though there might be physical restriction on the amount of drugs that can be administered. Using three *Lagrange multiplier* vectors, two of which are functions of space and time and one is independent of time, and letting $\mathbf{Z} = (\mathbf{Y}, \mathbf{U}, \boldsymbol{\xi}, \boldsymbol{\eta}, \boldsymbol{\chi})$ be an extended state vector, the *pseudo-Hamiltonian* is defined as,

$$\begin{aligned}\mathcal{H}(\mathbf{Z}) \equiv\ & \frac{1}{2}\int_0^{t_f} dt \int_\Omega d\mathbf{x} \left(\mathbf{Y}^\top R\mathbf{Y} + (\mathbf{U}-\mathbf{U}_0)^\top S\,(\mathbf{U}-\mathbf{U}_0)\right) \\ & + \frac{1}{2}\int_\Omega d\mathbf{x} \left(\mathbf{Y}^\top Q\mathbf{Y}\right)(\mathbf{x}, t_f) \\ & + \int_0^{t_f} dt \int_\Omega d\mathbf{x}\ \boldsymbol{\xi}^\top \Big(\mathbf{Y}_t - D\nabla_x^2[\mathbf{Y}] - (A+B)(\mathbf{Y})\mathbf{Y} - \mathbf{U}\Big) \\ & + \int_0^{t_f} dt \int_{\partial\Omega} d\boldsymbol{\Gamma}\ \boldsymbol{\eta}^\top \Big(-D\left(\widehat{\mathbf{N}} \cdot \nabla_x\right)[\mathbf{Y}]\Big) \\ & + \int_\Omega d\mathbf{x} \Big(\boldsymbol{\chi}^\top (\mathbf{Y} - \mathbf{Y}_0)\Big)(\mathbf{x}, 0).\end{aligned} \quad (6)$$

The *calculus of variations* is used to determine the functional critical point necessary condition for the first variation [4] of the *pseudo-Hamiltonian* $\mathcal{H}(\mathbf{Z})$. Let the perturbation $\delta\mathbf{Z}$ about the optimal trajectory $\mathbf{Z}^*$, be defined as $\delta\mathbf{Z} = \mathbf{Z} - \mathbf{Z}^*$. The pseudo-Hamiltonian is expanded as follows,

$$\mathcal{H}(\mathbf{Z}^* + \delta\mathbf{Z}) = \mathcal{H}(\mathbf{Z}^*) + \delta\mathcal{H}(\mathbf{Z}^*, \delta\mathbf{Z}) + O((\delta\mathbf{Z})^2).$$

The quadratic order terms, including the 2nd variation of $\mathcal{H}$ are neglected. In addition the functional dependence of the higher derivatives in time and state of the extended state perturbations must be eliminated on lower order terms by one or two integrations by parts, i.e., Green's formula. Merging these identities, rearranging inner products and collecting terms, the extended state equations yields the following intermediate form:

$$\begin{aligned}\delta\mathcal{H}(\mathbf{Z}^*, \delta\mathbf{Z}) = & \int_0^{t_f} dt \int_\Omega d\mathbf{x}\ \delta\mathbf{Y}^\top \big(R\mathbf{Y}^* - \boldsymbol{\xi}_t^* - \nabla_x^2[D\boldsymbol{\xi}^*] \\ & - (A+B)(\mathbf{Y}^*)\boldsymbol{\xi}^* - \nabla_Y[A+B](\mathbf{Y}^*) : (\boldsymbol{\xi}^*(\mathbf{Y}^*)^\top\big) \\ & + \int_0^{t_f} dt \int_\Omega d\mathbf{x}\ \delta\mathbf{U}^\top (S\,(\mathbf{U}^* - \mathbf{U}_0) - \boldsymbol{\xi}^*) \\ & + \int_0^{t_f} dt \int_\Omega d\mathbf{x}\ \delta\boldsymbol{\xi}^\top \big(\mathbf{Y}_t^* - D\nabla_x^2[\mathbf{Y}^*] \\ & - (A+B)(\mathbf{Y}^*)\mathbf{Y}^* - \mathbf{U}^*\big) \\ & - \int_0^{t_f} dt \int_{\partial\Omega} d\boldsymbol{\Gamma}\ \delta\boldsymbol{\eta}^\top D\left(\widehat{\mathbf{N}} \cdot \nabla_x\right)[\mathbf{Y}^*] \\ & + \int_0^{t_f} dt \int_{\partial\Omega} d\boldsymbol{\Gamma}\ \delta\mathbf{Y}^\top \left(\widehat{\mathbf{N}} \cdot \nabla_x\right)[D\boldsymbol{\xi}^*] \\ & - \int_0^{t_f} dt \int_{\partial\Omega} d\boldsymbol{\Gamma} \left(\widehat{\mathbf{N}} \cdot \nabla_x\right)\left[\delta\mathbf{Y}^\top\right] D(\boldsymbol{\eta}^* + \boldsymbol{\xi}^*) \\ & + \int_\Omega d\mathbf{x} \left(\delta\boldsymbol{\chi}^\top (\mathbf{Y}^* - \mathbf{Y}_0(\mathbf{x}))\right)(\mathbf{x}, 0) \\ & + \int_\Omega d\mathbf{x} \left(\delta\mathbf{Y}^\top (\boldsymbol{\chi}^* - \boldsymbol{\xi}^*)\right)(\mathbf{x}, 0) \\ & + \int_\Omega d\mathbf{x} \left(\delta\mathbf{Y}^\top (\boldsymbol{\xi}^* + Q\mathbf{Y}^*)\right)(\mathbf{x}, t_f),\end{aligned}$$

where $A : B$ denotes the trace of the matrix AB or the double-dot product, e.g., $\nabla_Y[A](\mathbf{Y}^*) : (\boldsymbol{\xi}^*(\mathbf{Y}^*)^\top = \sum_{j=1}^3 \sum_{k=1}^3 \nabla_Y[A_{j,k}]\xi_j^* Y_k^*$.

A. State Equations

The optimal state equation is recovered by setting the coefficient of $(\delta\boldsymbol{\xi})^\top$ to zero:

$$\mathbf{Y}_t^* = D\nabla_x^2[\mathbf{Y}^*] + (A+B)(\mathbf{Y}^*)\mathbf{Y}^* + \mathbf{U}^* \quad (7)$$

on $\Omega \times (0, t_f]$, with boundary conditions on $\partial\Omega \times [0, t_f]$ from the coefficient of $(\delta\boldsymbol{\eta})^\top$, i.e., $-D(\widehat{\mathbf{N}} \cdot \nabla_x)[\mathbf{Y}^*](\mathbf{x}, t) = \mathbf{0}$, for $(\mathbf{x}, t) \in \partial\Omega \times [0, t_f]$ and with initial conditions on the interior Ω from the coefficient of $(\delta\boldsymbol{\chi})^\top$, i.e., $\mathbf{Y}^*(\mathbf{x}, 0) = \mathbf{Y}_0(\mathbf{x})$ for $\mathbf{x} \in \Omega$. Due to the presence of the functions $A(\mathbf{Y})\mathbf{Y}$ and $B(\mathbf{Y})\mathbf{Y}$ the forward PDE (7) will be nonlinear.

B. Regular Optimal Control

Since the control has been defined in (3) as only having one component, only the coefficient of δU_3 is set to zero giving the corresponding regular control

$$U_3^*(\mathbf{x}, t) = U_{0,3}(\mathbf{x}, t) + \xi_3^*(\mathbf{x}, t)/s_3, \quad (8)$$

on $\Omega \times [0, t_f]$,provided $s_3 \neq 0$. Note that this control law only requires solving for the 3rd component of the first co-state vector $\boldsymbol{\xi}^*(\mathbf{x}, t)$, since $\delta U_1 \equiv 0$ and $\delta U_2 \equiv 0$.

C. Co-State Equations

Setting the functional coefficient of $(\delta\mathbf{Y})^\top$ to zero yields the primary co-state backward PDE:

$$\begin{aligned}\mathbf{0} = \boldsymbol{\xi}^*_t + \nabla_x^2[D\boldsymbol{\xi}^*] + (A+B)(\mathbf{Y}^*)\boldsymbol{\xi}^* \\ +\nabla_Y[A+B](\mathbf{Y}^*):(\boldsymbol{\xi}^*(\mathbf{Y}^*)^\top) - R\mathbf{Y}^*,\end{aligned} \tag{9}$$

for $(\mathbf{x},t) \in \Omega \times [0,t_f)$. This PDE (9) is unidirectionally coupled to the state PDE (7), except that only the 3rd component $\xi_3^*(\mathbf{x},t)$ is needed for the regular optimal control input $U_3^*(\mathbf{x},t)$ from (8). The boundary condition follows from setting the functional coefficient of $\delta\mathbf{Y}(\mathbf{x},t)$ for $\mathbf{x}$ on $\boldsymbol{\Gamma}=\partial\Omega$ to zero, so

$$(\widehat{\mathbf{N}}\cdot\nabla_x)[D\boldsymbol{\xi}^*](\mathbf{x},t) = \mathbf{0}, \quad (\mathbf{x},t) \in \partial\Omega \times [0,t_f) \tag{10}$$

and the final condition for this backward PDE follows from forcing the coefficient of $\delta\mathbf{Y}(\mathbf{x},t_f)$ to be zero on Ω,

$$\boldsymbol{\xi}^*(\mathbf{x},t_f) = -Q\mathbf{Y}^*(\mathbf{x},t_f). \tag{11}$$

The two other co-state vectors should not be needed, but satisfy rather simple equations. The 2nd co-state vector equation follows as the zero coefficient of $(\widehat{\mathbf{N}}\cdot\nabla_x)[\delta\mathbf{Y}^\top]$ on the state boundary $\boldsymbol{\Gamma}=\partial\Omega$, $\boldsymbol{\eta}^*(\mathbf{x},t) = -\boldsymbol{\xi}^*(\mathbf{x},t), \quad (\mathbf{x},t) \in \partial\Omega \times [0,t_f]$. The 3rd co-state vector equation follows as the zero coefficient of state initial condition $\delta\mathbf{Y}(\mathbf{x},0)$, $\boldsymbol{\chi}^*(\mathbf{x}) = \boldsymbol{\xi}^*(\mathbf{x},0), \quad \mathbf{x} \in \Omega$.

IV. Galerkin Finite Element Method

In an earlier paper [1] we had worked using a *Crank-Nicolson implicit method* to study the problem numerically. However, using finite difference methods like *Crank-Nicolson implicit method* and *alternating directions implicit method* have serious drawbacks. Finite difference techniques are more likely to have higher computational requirements, *i.e,* they suffer from the *curse of dimensionality*. Finite element methods require a relatively smaller number of nodes as compared to the finite difference methods while maintaining the same level of accuracy. Also, the finite element method can better handle irregular structure, such as the brain tumor. For the problem under consideration, we use the *Galerkin finite element method* so as to reduce the number of state nodes. The following steps can be used to get an approximate numerical solution using our predictor-corrector Crank-Nicolson adapted to finite element equations. Note that the assumption made in this paper is that the growth is *logistic* for the tumor and normal cells.

1) The first step ($\ell = 1$) would be to make a guess about the control $U_3^*(\mathbf{x},t) \simeq U_3^{(1)}(\mathbf{x},t)$. We substitute it into the forward state equations and use the finite element method to solve for the state $\mathbf{Y}^*(\mathbf{x},t) \simeq \mathbf{Y}^{(1)}(\mathbf{x},t)$ for $t > 0$. Initially, $\mathbf{Y}^*(\mathbf{x},0) = \mathbf{Y}_0(\mathbf{x})$. Let the Galerkin approximation for any state or control vector summarized in the global vector $\mathbf{Z}(\mathbf{x},t) = (\mathbf{Y},\mathbf{U}.\boldsymbol{\xi},\boldsymbol{\eta},\boldsymbol{\chi})$ be

$$\mathbf{Z}^*(\mathbf{x},t) \simeq \widehat{\mathbf{Z}}(\mathbf{x},t) \equiv \sum_{\hat{k}=1}^{M} \widehat{\mathbf{Z}}_{\hat{k}}(t) \cdot \phi_{\hat{k}}(\mathbf{x}), \tag{12}$$

where, $[\phi_i(\mathbf{x})]_{M\times 1}$, is a set of M linearly independent continuous basis functions, with the normalization property $\phi_{\hat{k}}(\mathbf{x}_{\hat{j}}) = \delta_{\hat{j},\hat{k}}$, at the element node $\mathbf{x}_{\hat{j}}$, implying the interpolation property that $\mathbf{Z}^*(\mathbf{x}_{\hat{j}},t) = \widehat{\mathbf{Z}}_{\hat{j}}(t)$ for $\hat{j} = 1{:}M$ finite element nodes.

2) Before applying the Galerkin approximation (12) to a state equation, say (7), the equation must be put into integral form on Ω with respect to a test function $\phi_{\hat{j}}(\mathbf{x})$ taken from the basis and then further prepared for low order basis function by reducing the 2nd order derivatives to 1st order derivatives by integration by parts i.e., again by Green's formula, so

$$\begin{aligned}\mathbf{0} &= \int_\Omega d\mathbf{x}\phi_{\hat{j}}(\mathbf{x})\left(\mathbf{Y}^*_t - D\nabla_x^2[\mathbf{Y}^*] - (A+B)(\mathbf{Y}^*)\mathbf{Y}^* - \mathbf{U}^*\right) \\ &= \int_\Omega d\mathbf{x}\left(\phi_{\hat{j}}\mathbf{Y}^*_t + D\nabla_x^\top[\phi_{\hat{j}}]\nabla_x[\mathbf{Y}^*]\right. \\ &\quad \left. -\phi_{\hat{j}}\left((A+B)(\mathbf{Y}^*)\mathbf{Y}^* + \mathbf{U}^*\right)\right),\end{aligned}$$

for $\hat{j} = 1:M$, where the exact no-flux boundary condition has been used in the last step.

3) Application of the Galerkin approximation (12) yields

$$\begin{aligned}\mathbf{0} \simeq \sum_{\hat{k}=1}^{M} \int_\Omega d\mathbf{x}\left(\widehat{\mathbf{Y}}'_{\hat{k}}\phi_{\hat{j}}\phi_{\hat{k}} + D\widehat{\mathbf{Y}}_{\hat{k}}\left(\nabla_x^\top[\phi_{\hat{j}}]\nabla_x[\phi_{\hat{k}}]\right)\right. \\ \left. -\left((A+B)\left(\widehat{\mathbf{Y}}\right)\widehat{\mathbf{Y}}_{\hat{k}} + \widehat{\mathbf{U}}_{\hat{k}}\right)\phi_{\hat{j}}\phi_{\hat{k}}\right),\end{aligned}$$

for $\hat{j} = 1 : M$. Futher reduction to finite element integrals is accomplished by letting

$$\mathcal{M}_{\hat{j},\hat{k}} \equiv \int_\Omega d\mathbf{x}\phi_{\hat{j}}(\mathbf{x})\phi_{\hat{k}}(\mathbf{x}) \tag{13}$$

be an element mass integral for $\hat{j},\hat{k} = 1 : M$,

$$\mathcal{K}_{\hat{j},\hat{k}} \equiv \int_\Omega d\mathbf{x}\nabla_x^\top[\phi_{\hat{j}}]\nabla_x[\phi_{\hat{k}}] \tag{14}$$

be an element stiffness integral for $\hat{j},\hat{k} = 1 : M$, and

$$\mathcal{T}_{\hat{j},\hat{k},\hat{l}} \equiv \int_\Omega d\mathbf{x}\phi_{\hat{j}}(\mathbf{x})\phi_{\hat{k}}(\mathbf{x})\phi_{\hat{l}}(\mathbf{x}) \tag{15}$$

be a triple basis element integral for $\hat{j},\hat{k},\hat{l} = 1 : M$ arising from the purely nonlinear terms in $A(\mathbf{Y})\mathbf{Y}$ and $B(\mathbf{Y})\mathbf{Y}$. Thus, the Galerkin equation becomes

$$\begin{aligned}\mathbf{0} = \sum_{\hat{k}=1}^{M}\left(\mathcal{M}_{\hat{j},\hat{k}}\left(\widehat{\mathbf{Y}}'_{\hat{k}}(t) - \left(a_1\mathbf{e}_1\mathbf{e}_1^\top + a_2\mathbf{e}_2\mathbf{e}_2^\top\right.\right.\right. \\ \left.\left.\left. -a_3\mathbf{e}_3\mathbf{e}_3^\top\right)\widehat{\mathbf{Y}}_{\hat{k}}(t) - \widehat{\mathbf{U}}_{\hat{k}}(t)\right) + \mathcal{K}_{\hat{j},\hat{k}}D\widehat{\mathbf{Y}}_{\hat{k}}(t) \\ + \sum_{\hat{l}=1}^{M}\mathcal{T}_{\hat{j},\hat{k},\hat{l}}\left(\frac{a_1}{k_1}\widehat{Y}_{1,\hat{k}}(t)\widehat{Y}_{1,\hat{l}}(t)\mathbf{e}_1 + \frac{a_2}{k_2}\widehat{Y}_{2,\hat{k}}(t)\widehat{Y}_{2,\hat{l}}(t)\mathbf{e}_2\right. \\ + \left(\alpha_{1,2}\widehat{Y}_{2,\hat{l}}(t) + \kappa_{1,3}\widehat{Y}_{3,\hat{l}}(t)\right)\widehat{Y}_{1,\hat{k}}(t)\mathbf{e}_1 \\ \left. + \left(\alpha_{2,1}\widehat{Y}_{1,\hat{l}}(t) + \kappa_{2,3}\widehat{Y}_{3,\hat{l}}(t)\right)\widehat{Y}_{2,\hat{k}}(t)\mathbf{e}_2\right)\Big),\end{aligned} \tag{16}$$

for $\hat{j} = 1 : M$. This Galerkin ODE can be solved by approximating the Galerkin basis integral coefficients $(\mathcal{M}_{\hat{j},\hat{k}}, \mathcal{K}_{\hat{j},\hat{k}}, \mathcal{T}_{\hat{j},\hat{k},\hat{l}})$ by exact symbolic methods or numerical quadrature if there is sufficient element

complexity, and then the ODE can be solved by our predictor-corrector Crank-Nicolson method [1] adapted to finite element equations. The coefficients can be computed for all double shots for fixed finite elements off-line since they will be fixed. These coefficients can be calculated on an element-by-element decomposition and element results can later be reassembled to form the global solution [7].

4) In the second shot of the double shot algorithm [1], the final condition (11),

$$\boldsymbol{\xi}^{(\ell)}(\mathbf{x},t_f) \simeq -Q\sum_{\hat{k}=1}^{M}\widehat{\mathbf{Y}}_{\hat{k}}^{(\ell)}(t_f)\phi_{\hat{k}}(\mathbf{x}),$$

for $\ell = 1:L$ double shots, is used to start the backward co-state solution. Similar to the state equation, a Galerkin approximation for the co-state equation (after dropping the (ℓ) subscript) using the same basis is given by (12) for $t < t_f$. As with the state Galerkin variational formulation, the variation formulation for the co-state equation (9) is

$$\begin{aligned}\mathbf{0} &= \int_\Omega d\mathbf{x}\phi_{\hat{j}}(\mathbf{x})\left(\boldsymbol{\xi}_t^*+\nabla_x^2[D\boldsymbol{\xi}^*]+(A+B)(\mathbf{Y}^*)\boldsymbol{\xi}^*\right.\\ &\quad\left.+\nabla_Y[A+B](\mathbf{Y}^*):(\boldsymbol{\xi}^*(\mathbf{Y}^*)^\top)-R\mathbf{Y}^*\right)\\ &= \int_\Omega d\mathbf{x}\left(\phi_{\hat{j}}\left(\boldsymbol{\xi}_t^*+(A+B)(\mathbf{Y}^*)\boldsymbol{\xi}^*\right.\right.\\ &\quad\left.+\nabla_Y[A+B](\mathbf{Y}^*):(\boldsymbol{\xi}^*(\mathbf{Y}^*)^\top)-R\mathbf{Y}^*\right)\\ &\quad\left.-\nabla_x^\top[\phi_{\hat{j}}]\nabla_x[D\boldsymbol{\xi}^*]\right)+\int_{\partial\Omega}d\Gamma\phi_{\hat{j}}\left(\widehat{\mathbf{N}}\cdot\nabla_x\right)[D\boldsymbol{\xi}^*].\end{aligned}$$

A form with reduced order derivatives is derived by eliminating the boundary integral by the no-flux condition (10) and then the Galerkin approximations are substituted for the state and co-state, thus producing

$$\begin{aligned}\mathbf{0} \simeq \sum_{\hat{k}=1}^{M}\int_\Omega d\mathbf{x}\left(\left(\widehat{\boldsymbol{\xi}}'_{\hat{k}}(t)+(A+B)(\widehat{\mathbf{Y}})\widehat{\boldsymbol{\xi}}_{\hat{k}}\right.\right.\\ \left.+\nabla_Y[A+B](\widehat{\mathbf{Y}}):(\widehat{\boldsymbol{\xi}}_{\hat{k}}(\widehat{\mathbf{Y}})^\top)-R\widehat{\mathbf{Y}}_{\hat{k}}\right)\phi_{\hat{j}}\phi_{\hat{k}}\\ \left.-D\widehat{\boldsymbol{\xi}}_{\hat{k}}\nabla_x^\top[\phi_{\hat{j}}]\nabla_x[\phi_{\hat{k}}]\right),\end{aligned}$$

for $\hat{j} = 1:M$. Next by substituting the Galerkin approximation for $\widehat{\mathbf{Y}}$ in the nonlinear terms, using the element Galerkin integral notation for the mass $\mathcal{M}_{\hat{j},\hat{k}}$ (13), stiffness $\mathcal{K}_{\hat{j},\hat{k}}$ (14) and the pure nonlinear triple $\mathcal{T}_{\hat{j},\hat{k},\hat{l}}$ (15), the compact Galerkin ODEs are obtained:

$$\begin{aligned}\mathbf{0} = \sum_{\hat{k}=1}^{M}\left(\mathcal{M}_{\hat{j},\hat{k}}\left(\widehat{\boldsymbol{\xi}}'_{\hat{k}}(t)+a_1\widehat{\xi}_{1,\hat{k}}\mathbf{e}_1+a_2\widehat{\xi}_{2,\hat{k}}\mathbf{e}_2\right.\right.\\ \left.-a_3\widehat{\xi}_{3,\hat{k}}\mathbf{e}_3-R\widehat{\mathbf{Y}}_{\hat{k}}(t)\right)-\mathcal{K}_{\hat{j},\hat{k}}D\widehat{\boldsymbol{\xi}}_{\hat{k}}(t)\\ -\sum_{\hat{l}=1}^{M}\mathcal{T}_{\hat{j},\hat{k},\hat{l}}\left(\frac{2a_1}{k_1}\widehat{Y}_{1,\hat{l}}(t)\widehat{\xi}_{1,\hat{k}}(t)\mathbf{e}_1+\frac{2a_2}{k_2}\widehat{Y}_{2,\hat{l}}(t)\widehat{\xi}_{2,\hat{k}}(t)\mathbf{e}_2\right.\\ +\alpha_{1,2}\left(\widehat{Y}_{2,\hat{l}}(t)\mathbf{e}_1+\widehat{Y}_{1,\hat{l}}(t)\mathbf{e}_2\right)\widehat{\xi}_{1,\hat{k}}(t)\\ +\kappa_{1,3}\left(\widehat{Y}_{3,\hat{l}}(t)\mathbf{e}_1+\widehat{Y}_{1,\hat{l}}(t)\mathbf{e}_3\right)\widehat{\xi}_{1,\hat{k}}(t)\\ +\alpha_{2,1}\left(\widehat{Y}_{2,\hat{l}}(t)\mathbf{e}_1+\widehat{Y}_{1,\hat{l}}(t)\mathbf{e}_2\right)\widehat{\xi}_{1,\hat{k}}(t)\\ \left.\left.+\kappa_{2,3}\left(\widehat{Y}_{3,\hat{l}}(t)\mathbf{e}_2+\widehat{Y}_{2,\hat{l}}(t)\mathbf{e}_3\right)\widehat{\xi}_{2,\hat{k}}(t)\right)\right),\end{aligned}\tag{17}$$

for $\hat{j} = 1:M$. This Galerkin ODE (17) may be computed by the appropriate numerical methods using the same Galerkin integral basis coefficients.

5) For each completed double shot for $\ell = 1:L$, the co-state approximation $\widehat{\boldsymbol{\xi}}^{(\ell)}(\mathbf{x},t) = \sum_{\hat{k}=1}^{M}\widehat{\boldsymbol{\xi}}_{\hat{k}}^{(\ell)}(t)\phi_{\hat{k}}(\mathbf{x})$ is used to determine the *regular optimal control* (8) updated value third component

$$\widehat{U}_3^{(\ell+1)}(\mathbf{x},t) = U_{0,3}(\mathbf{x},t)+\widehat{\xi}_3^{(\ell)}(\mathbf{x},t)/s_3.$$

6) This process is repeated for $\ell = 2:L$ double shot iterations until a convergence criterion for sufficiently large L is reached, e.g., the relative criterion for the control,

$$\begin{aligned}\left|\left|U_3^{(\ell)}(\mathbf{x},t)-U_3^{(\ell-1)}(\mathbf{x},t)\right|\right| &< \mathrm{tol}_u\left|\left|U_3^{(\ell-1)}(\mathbf{x},t)\right|\right|,\\ \left|\left|\mathbf{Y}^{(\ell)}(\mathbf{x},t)-\mathbf{Y}^{(\ell-1)}(\mathbf{x},t)\right|\right| &< \mathrm{tol}_y\left|\left|\mathbf{Y}^{(\ell-1)}(\mathbf{x},t)\right|\right|,\end{aligned}$$

for $\ell = 2{:}L$ until satisfied, provided $||U_3^{(\ell-1)}(\mathbf{x},t)|| \neq 0$ and $||\mathbf{Y}^{(\ell-1)}(\mathbf{x},t)|| \neq 0$, where $\mathrm{tol}_u > 0$ and $\mathrm{tol}_y > 0$ are some prescribed tolerances.

V. Polar Finite Element Test Configuration

Consider two-dimensional configuration that is a circular disk of radius R_r with center at the origin. Transforming the rectangular space coordinates $(x,y) = r(\cos(\theta),\sin(\theta))$ to polar coordinates permits use of a completely covering rectangular grid configuration in the $r\theta$-plane and is consistent with the v ariational representation of no-flux boundary condition. The grid is contructed of M_s sectors of angular width $\Delta\theta{=}2\pi/M_s$ and each sector is further partitioned into M_r subsectors of radial length $\Delta r{=}R_r/M_r$. The nodes are given by $(\theta_{\hat{i}}, r_{\hat{j}}){=}((\hat{i}-1)\Delta\theta,(\hat{j}-1)\Delta r)$ for $\hat{i}{=}1:M_s{+}1$ and $\hat{j}{=}1:M_r{+}1$. Due to the one-to-many properties of the transformation, all $r{=}r_1{=}0$ nodes are aliased to the first global node numbered 1, while all $\theta{=}\theta_{M_s+1}{=}2\pi$ nodes are aliased to the corresponding global node with $\theta{=}\theta_1{=}0$ and the same $r{=}r_{\hat{j}}$ for $\hat{j}{=}1:M_r{+}1$. Otherwise, the global node numbering is given by $n_{\hat{k}}{=}\hat{i}{+}\,(\hat{j}-1){*}M_s$ for $\hat{i}{=}1:M_s$ and for $\hat{j}{=}1:M_r{+}1$, corresponding to column (θ) ordering and aliasing for $\hat{i}{=}M_s$. The elements are similarly numbered as $e_{\hat{i},\hat{j}}{=}\hat{i}{+}(\hat{j}-1){*}M_s$ for $\hat{i}{=}1:M_s$ and for $\hat{j}{=}1:M_r$, while the element local node numbering is $k_e = 1{:}4$ in the clockwise direction, going first along the $r{=}r_{\hat{j}}$ edge, see Figure 1 showing the relationship between local and global node numbering.

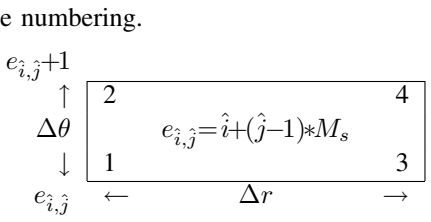

Fig. 1. Typical finite element configuration in $r\theta$-plane.

Though the configuration may seem complex, it greatly facilitates the deassembly and reassembly between the elements locally to the global representation, while allowing

one system to define the approximating basis functions for all elements except for the elements adjacent to the origin.

For simplicity, bilinear quadrilateral basis functions are used for the non-origin elements, where for element $e_{\hat{i},\hat{j}}$ on $(\theta_{\hat{i}},\theta_{\hat{i}_{+}1})\times(r_{\hat{j}},r_{\hat{j}+1})$ for $\hat{i}{=}1:M_s+1$ and for $\hat{j}{=}2:M_r$ in the $k_e=1{:}4$ element node numbering,

$$\phi_1^{(\hat{i},\hat{j})}(r,\theta) = \left(\frac{\theta_{\hat{i}+1}-\theta}{\Delta\theta}\right)\left(\frac{r_{\hat{j}+1}-r}{\Delta r}\right); \tag{18}$$

$$\phi_2^{(\hat{i},\hat{j})}(r,\theta) = \left(\frac{\theta-\theta_{\hat{i}}}{\Delta\theta}\right)\left(\frac{r_{\hat{j}+1}-r}{\Delta r}\right); \tag{19}$$

$$\phi_3^{(\hat{i},\hat{j})}(r,\theta) = \left(\frac{\theta_{\hat{i}+1}-\theta}{\Delta\theta}\right)\left(\frac{r-r_{\hat{j}}}{\Delta r}\right); \tag{20}$$

$$\phi_4^{(\hat{i},\hat{j})}(r,\theta) = \left(\frac{\theta-\theta_{\hat{i}}}{\Delta\theta}\right)\left(\frac{r-r_{\hat{j}}}{\Delta r}\right), \tag{21}$$

else zero outside the element $(\hat{i},\hat{j})$. For the elements when $\hat{j}=1$ the basis functions for local nodes $k_e=3:4$ are still valid, but the $k_e=2$ nodes for $r_1=0$ are aliases for the $k_e=1$ nodes since all $r_1=0$ nodes must have the same values, so we need the basis functions for triangular elements $k_e=1,3,4$ to be consistent with the circular sector in cartesian coordinates, so $\phi_1^{(\hat{i},1)}(r,\theta)=1-r/\Delta r$; replaces (18) for $k_e=1$ and (19) for $k_e=2$ is not used, while (20) for $k_e=3$ and (21) for $k_e=4$, respectively, are still valid.

The element version of the global mass matrix (13) is

$$\widehat{\mathcal{M}}_{i_e,j_e}^{(\hat{i},\hat{j})}=\int_{\theta_{\hat{i}}}^{\theta_{\hat{i}+1}}d\theta\int_{r_{\hat{j}}}^{r_{\hat{j}+1}}drr\phi_{i_e}^{(\hat{i},\hat{j})}(r,\theta)\phi_{j_e}^{(\hat{i},\hat{j})}(r,\theta),$$

for local node numbers $i_e,j_e=1:4$, and produces the symmetric $(\hat{i},\hat{j})$ non-origin element matrix

$$\widehat{\mathcal{M}}^{(\hat{i},\hat{j})}=\frac{(\Delta r)^2\Delta\theta}{72}\begin{bmatrix}2(4\hat{j}{-}3) & (4\hat{j}{-}3) & 2(2\hat{j}{-}1) & (2\hat{j}{-}1)\\ * & 2(4\hat{j}{-}3) & (2\hat{j}{-}1) & 2(2\hat{j}{-}1)\\ * & * & 2(4\hat{j}{-}1) & (4\hat{j}{-}1)\\ * & * & * & 2(4\hat{j}{-}1)\end{bmatrix},$$

where the symmetric lower triangular components have been suppressed $(*)$. Note that the corresponding element area is $\mathcal{A}^{(\hat{i},\hat{j})}=(\Delta r)^2\Delta\theta(2\hat{j}-1)/2$. Using the rectangular-polar gradient identity, $\nabla_x^\top[\phi_i]\nabla_x[\phi_j]{=}\phi_{i,r}\phi_{j,r}{+}\phi_{i,\theta}\phi_{j,\theta}/r^2$, the element version of the global stiffness matrix (13) is

$$\widehat{\mathcal{K}}_{i_e,j_e}^{(\hat{i},\hat{j})}=\int_{\theta_{\hat{i}}}^{\theta_{\hat{i}+1}}d\theta\int_{r_{\hat{j}}}^{r_{\hat{j}+1}}drr\left(\phi_{i_e,r}^{(\hat{i},\hat{j})}\phi_{j_e,r}^{(\hat{i},\hat{j})}{+}\phi_{i_e,\theta}^{(\hat{i},\hat{j})}\phi_{j_e,\theta}^{(\hat{i},\hat{j})}/r^2\right)(r,\theta)$$

and produces the symmetric $(\hat{i},\hat{j})$ element matrix

$$\begin{aligned}\widehat{\mathcal{K}}^{(\hat{i},\hat{j})} &= \frac{(2\hat{j}{-}1)\Delta\theta}{12}\begin{bmatrix}+2 & +1 & -2 & -1\\ * & +2 & -1 & -2\\ * & * & +2 & +1\\ * & * & * & +2\end{bmatrix}\\ &= +\frac{\ln\left(\frac{\hat{j}}{\hat{j}-1}\right)}{2\Delta\theta}\begin{bmatrix}+2\hat{j}^2 & -2\hat{j}^2 & -2\hat{j}(\hat{j}{-}1) & +2\hat{j}(\hat{j}{-}1)\\ * & +2\hat{j}^2 & +2\hat{j}(\hat{j}{-}1) & -2\hat{j}(\hat{j}{-}1)\\ * & * & +2(\hat{j}{-}1)^2 & -2(\hat{j}{-}1)^2\\ * & * & * & +2(\hat{j}{-}1)^2\end{bmatrix}\\ &= +\frac{1}{2\Delta\theta}\begin{bmatrix}-(2\hat{j}+1) & +(2\hat{j}+1) & +(2\hat{j}{-}1) & -(2\hat{j}{-}1)\\ * & -(2\hat{j}+1) & -(2\hat{j}{-}1) & +(2\hat{j}{-}1)\\ * & * & -(2\hat{j}{-}3) & +(2\hat{j}{-}3)\\ * & * & * & -(2\hat{j}{-}3)\end{bmatrix},\end{aligned}$$

where again the symmetric lower triangular components have been suppressed $(*)$. The triple basis coefficient (15) of the nonlinear terms is a $4\times4\times4$ array on each element,

$$\widehat{\mathcal{T}}_{i_e,j_e,k_e}^{(\hat{i},\hat{j})}=\int_{\theta_{\hat{i}}}^{\theta_{\hat{i}+1}}d\theta\int_{r_{\hat{j}}}^{r_{\hat{j}+1}}drr\phi_{i_e}^{(\hat{i},\hat{j})}(r,\theta)\phi_{j_e}^{(\hat{i},\hat{j})}(r,\theta)\phi_{k_e}^{(\hat{i},\hat{j})}(r,\theta),$$

so the actual values are omitted due to lack of space. Other element coefficient matrices, such as those for the elements adjacent to the origin, are also omitted due to lack of space.

VI. Computational Results

The double shot, forward and backward iteration algorithm using the finite element method outlined in Section IV was implemented on the two-dimensional space with the three states and the drug input control. The numerical implementation of the algorithm is adapted to finite element equations from our one space dimension application in [1], except there the finite difference version of Crank-Nicolson's method was used and is too costly to extend to another dimension.

The data for the numerical parameters are drawn from various sources including Wang et al. [9], [10], Swanson[8] and Murray [6], while unavailable parameters were estimated. The diffusion diagonal vector is D = [4.2e-3, 1.e-15,0.22] cm^2 per day. The quadratic cost coefficients are $r_1=q_1=q_3=0.1$ and $s_3=0.2$. The net growth coefficient is a = [1.2e-2, 8.6e-7, 11.1] per day. The other coefficients are $k_i=1$ for $i=1:2$, $\alpha_{1,2}=\alpha_{2,1}=\kappa_{2,3}=$ 1.e-4 and $\kappa_{1,3}=0.5$. Following Murray, the initial state for the normal tissue is assumed to be uniformly one. The initial tumor spread and drug concentration are assumed to be Gaussian with mean 0, spread 0.2 and weights 1.0e-3 and 0.15, respectively. Maple 9.5 was used to exactly evaluate the integrals of the element matrices.

The main advantage of the polar coordinate FEM formulation is that the no-flux boundary condition (4) is implicit in the method when the domain is our test circle. The penalty for this advantage is the nonuniqueness of the origin (for any θ when $r=0$) and for the branch cut along the positive x-axis. The non-unique alias nodes were eliminated leading to a reduction in the number of vector ODEs in the time t. These ODEs where treated by an efficient finite element variant of our predictor-corrector *Crank-Nicolson* method that uses a predictor-corrector method to handle the nonlinear terms and higher space dimensions. The state and co-state are discretized at the forward and backward mid-point in time, respectively, and the algorithm is implemented in MATLAB. The Crank-Nicolson temporal mid-point was approximated by $\mathbf{Y}_{\mathbf{j},k+0.5}^{(\gamma,\ell)}=0.5*\left(\mathbf{Y}_{\mathbf{j},k+1}^{(\gamma,\ell)}+\mathbf{Y}_{\mathbf{j},k}^{(\ell)}\right)$, for vector node index $\mathbf{j}$, time index k, double shot ℓ and correction γ. The FEM ODE is discretized in the general form

$$\widehat{A}_{km}(\widehat{\mathbf{Y}}_{k+1}-\widehat{\mathbf{Y}}_k)=\widehat{B}_{km}\widehat{\mathbf{Y}}_k+dt\mathcal{M}\widehat{\mathbf{U}}_{km}$$

and solved by the MATLAB built-in backslash 'method. Similar discretization and approximation was used for the co-state equations. The Fig. 2 shows a sample history of the tumor density $Y_1(r,\pi,t)$ on the interval $r\in[-5,5]$

over a $T = 5$ day treatment schedule for the quartiles in time $t = 0, 1.25, 2.5, 3.75, 5.0$. For this test case the distribution of the tumor using the optimal drug delivery showed a significant reduction of 51.3 percent of the total tumor density integral over the 5 day treatment period. The time taken by the program was 32.8 minutes.

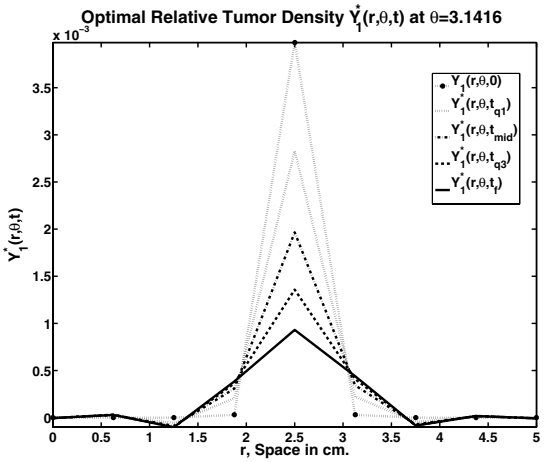

Fig. 2. The optimal, relative tumor density $Y_1^*(r, \theta, t)$ versus r parametrized in time, $t = 0, 1.25, 2.5, 3.75, 5.0$ days, as a cross-section at $\theta = \pi$, the original tumor density peak location with $r = 2.5$ also. The polar grid size is $(M_r, M_s) = (8, 6)$.

A more detailed presentation of the final tumor density is given in Fig. 3 over the (r, θ) plane at $T = 5$ days showing that although the peak value is small, the tumor has spread through most of the plane.

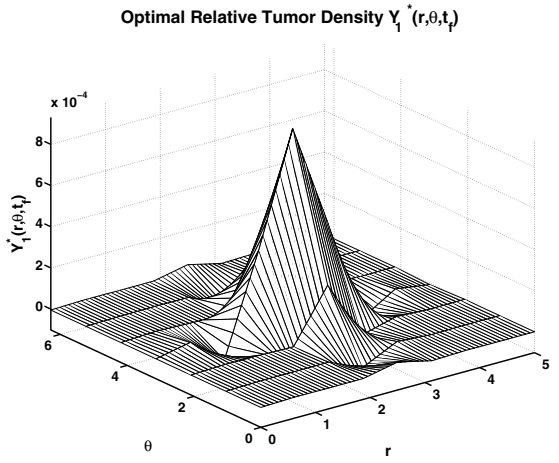

Fig. 3. The final optimal, relative tumor density $Y_1^*(r, \theta, t)$ over $(r, theta)$ plane at time $t = T = 5.0$ days. The FEM polar grid size is $(M_r, M_s) = (8, 6)$, but a grid refinement is presented by using the FEM basis as an interpolant.

VII. Conclusion and Future Directions

The theory of Galerkin finite elements is used to develop approximations to the distributed parameter optimal control problem of cancer drug delivery to the brain governed by a coupled set of three reaction diffusion PDEs. The three state variables are the tumor cell density, the normal cell density and the cancer drug concentration. The tumor and normal cells are highly coupled through intrinsic and competitive interactions, the concentration is directly controlled by the drug delivery control rate. The optimally controlled distributed parameter system is derived by a straight-forward calculus of variations technique without resort to an extremely abstract formulation, and that should be useful in other similar scientific or engineering applications.

The system of optimal PDEs in six state dimensions is reduced by Galerkin approximations of the state, co-state and control vectors to a system of six ODEs in time with three fundamental element integral coefficient forms: the mass, the stiffness and nonlinear coefficients. The finite element configuration is given for a circular disk geometry that can be used to test the optimal drug delivery computations. This finite element configuration will be more amenable to complex brain structures and three-dimensional geometries than the finite difference method of our earlier work.

Future directions include:

- Application to multidimensional drug delivery domains;
- Application to general curvilinear coordinates for general brain geometries;
- Application to heterogeneous brain structures such as spinal fluid cavities, variable brain matter, vascular system and the blood brain barrier.

VIII. Acknowledgments

The authors gratefully acknowledge Dr. Herbert H. Engelhard of Neurological Surgery at the University of Illinois Medical Center for suggesting the problem and Professor William D. O'Neill of Bioengineering at the University of Illinois at Chicago for putting us in contact.

References

[1] S. P. Chakrabarty and F. B. Hanson,"Optimal control of drug delivery to brain tumors for a distributed parameters model," in *Proceedings of American Control Conference*, pp. 973-978, June 2005.

[2] H. H. Engelhard, "Brain Tumors and the Blood-Brain Barrier," *Neuro-Oncology, The Essentials*, pp. 49-53, Thieme Medical Publishers, Inc., New York 2000.

[3] R. A. Gatenby and E. T. Gawlinski, "A Reaction-Diffusion Model of Cancer Invasion," *Cancer Research*, vol. 56, pp. 5745-5753, December 15, 1996.

[4] M. D. Gunzburger, *Perspectives in Flow Control and Optimization*, SIAM Series in Design and Control, Philadelphia, 2003.

[5] J. Mansuri, *The Modelling of Tumor Growth Using Reaction-Diffusion Equations*, MSc Thesis, Oxford University, 2002.

[6] J. D. Murray, *Mathematical Biology II: Spatial Models and Biomedical Applications*, Springer, New York, 2003.

[7] G. Sewell, *The Numerical Solution of Ordinary and Partial Differential Equations*, Academic Press, New York, 1988.

[8] K. R. Swanson, *Mathematical Modeling of the Growth and Control of Tumors*, PhD Thesis, University of Washington, 1999.

[9] C-H. Wang and J. Li, "Three dimensional simulation of IgG delivery to tumors," *Chemical Engineering Science*, vol. 53, pp. 3579-3600, 1998.

[10] C-H. Wang, J. Li, C. S. Teo and T. Lee, "The delivery of BCNU to brain tumors," *Journal of Controlled Release*, vol. 61, pp. 21-41, 1999.

[11] J. J. Westman, B. R. Fabijonas, D. L. Kern and F. B. Hanson, "Probabilistic Rate Compartment Cancer Model: Alternate versus Traditional Chemotherapy Scheduling," in *Stochastic Theory and Control*, *Lecture Notes in Control and Information Sciences*, vol. 280, B. Pasik-Duncan (Editor), Springer-Verlag, New York, pp. 491-506, 2002.